Some Properties of $LaNi_{5-x}Al_x$ Metal Alloys and the Diffusion Coefficient and Solubility of Hydrogen in Cyclohexane

Erwin D. Snijder, Geert F. Versteeg,* and Wim P. M. van Swaaij

Department of Chemical Engineering, Twente University of Technology, P.O. Box 217, 7500 AE Enschede, The Netherlands

Pressure–composition isotherms for hydrogen absorption and desorption have been measured for several alloys of the $LaNi_{5-x}Al_x$ family at 298, 308, 323, 333, and 348 K, and the $\Delta H°$ and $\Delta S°$ of the hydride formation reaction were obtained. The equilibrium pressure is strongly related to the aluminum content in the alloy. Other specific properties which have been determined are the density of the metal alloys and the particle size distribution and surface area of the material after about 50 absorption/desorption cycles with pure hydrogen. Additionally, the solubility and the diffusion coefficient of hydrogen in cyclohexane have been measured, and the solubility of hydrogen in ethanol has been correlated with results available in the literature.

1. Introduction

For a complete understanding of the mechanism of hydrogen absorption and desorption in or from metal hydride slurries, the physicochemical properties of the hydrides and the solvents need to be known. Although the equilibrium pressures of most metal hydrides can be found in the literature, discrepancies between the various data sources occur. This can most likely be attributed to small differences in alloy composition. Also, inhomogeneities can be introduced during the production when the alloys are not thoroughly mixed (*1*, *2*). These factors mainly affect the thermodynamic properties of the material (equilibrium pressures and the sloping of the plateau). Consequently, they have to be determined for every individual batch metal alloy. In the present study several properties of the $LaNi_{5-x}Al_x$ alloys as applied by Snijder *et al.* (*3*, *4*) have been measured. The physical properties of the solvents they used, cyclohexane and ethanol, were partly available in the literature (vapor pressure and density of both solvents, hydrogen solubility in ethanol). The remaining properties, the solubility and diffusion coefficient of hydrogen in cyclohexane, have been measured in the present work.

The metal alloys $LaNi_{4.5}Al_{0.5}$, $LaNi_{4.6}Al_{0.4}$, $LaNi_{4.7}Al_{0.3}$, $LaNi_{4.8}Al_{0.2}$, and $LaNi_5$ were supplied by Japan Metals & Chemicals (JMC), and $LaNi_{4.9}Al_{0.1}$ was obtained from Highways International. Cyclohexane has been provided by Merck (≥99.9%) and hydrogen by Hoekloos (≥99.999%).

2. Properties of $LaNi_{5-x}Al_x$ Hydride-Forming Metal Alloys

2.1. Pressure–Composition Isotherms. Figure 1 shows the experimental setup which has been applied for the determination of pressure–composition isotherms (PCT curves). The reactor (volume 568 cm^3) is kept at a constant temperature by means of external heating/cooling with an oil bath. Via a pressure reduce valve the reactor is connected with a hydrogen storage vessel (volume 1068 cm^3) and with a second vessel (volume 4610 cm^3) which can be evacuated. Between both vessels and the reactor is situated a magnetic valve. The experiments were carried out with about 50–75 g of metal powder in the reactor. After the addition of the alloy into the reactor, the reactor was evacuated (0.1 mbar) for several hours, whereafter about 15 absorption (at 25 bar)/desorption (at 0.1 mbar) cycles were carried out, all at 333 K. The hydrogen absorption capacity then reached a final and maximum value (F_{max}), which is a function of the aluminum content and temperature.

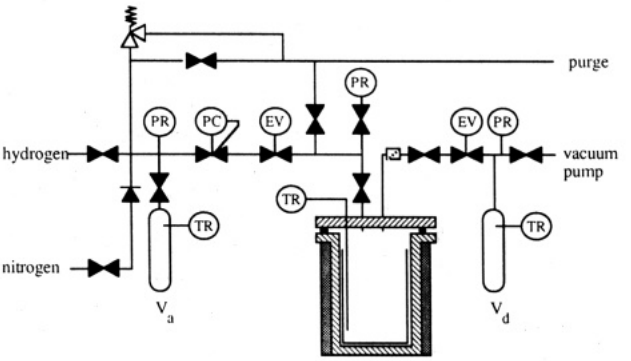

Figure 1. Experimental setup for the determination of the pressure–composition isotherms.

Table 1. Thermodynamic Data, Change in Enthalpy at Standard Pressure, $\Delta H°$, and Change in Entropy at Standard Pressure, $\Delta S°$, of the Hydride-Forming Metal Alloys

	absorption		desorption	
material	$\Delta H°$/ ($J \cdot mol^{-1} \cdot K^{-1}$)	$\Delta S°$/ ($kJ \cdot mol^{-1} \cdot K^{-1}$)	$\Delta H°$/ ($J \cdot mol^{-1} \cdot K^{-1}$)	$\Delta S°$/ ($kJ \cdot mol^{-1} \cdot K^{-1}$)
$LaNi_{4.5}Al_{0.5}$	−39.45	−115.1		
$LaNi_{4.6}Al_{0.4}$	−37.85	−114.5		
$LaNi_{4.7}Al_{0.3}$	−35.23	−110.7		
$LaNi_{4.8}Al_{0.2}$	−33.38	−110.7	35.66	113.7
$LaNi_{4.9}Al_{0.1}$	−31.73	−111.6	33.16	113.2
$LaNi_5$	−31.28	−111.3	31.93	111.5

Before an absorption experiment, the reactor was completely evacuated (0.1 mbar). After the supply of a small amount of hydrogen to the reactor (shortly opening the magnetic valve), equilibrium was allowed to establish. The temperature and pressure both in the reactor and storage vessel were recorded; next, a new amount of hydrogen was supplied to the reactor. This was repeated until the maximum pressure was reached. The desorption curves were then obtained by repeatedly venting small amounts of hydrogen through the magnetic valve into the desorption vessel. After reaching equilibrium, the temperature and pressure in the reactor and in the initially evacuated desorption storage vessel were measured.

From the pressure and temperature in the reactor and storage vessel and the amount of metal alloy in the reactor, the hydrogen absorption capacity F can be calculated. In Figure 2 the PCT curves for $LaNi_{4.8}Al_{0.2}$ are shown; similar results were obtained for $LaNi_{4.9}Al_{0.1}$ and $LaNi_5$, respectively.

0021-9568/94/1739-0405$04.50/0

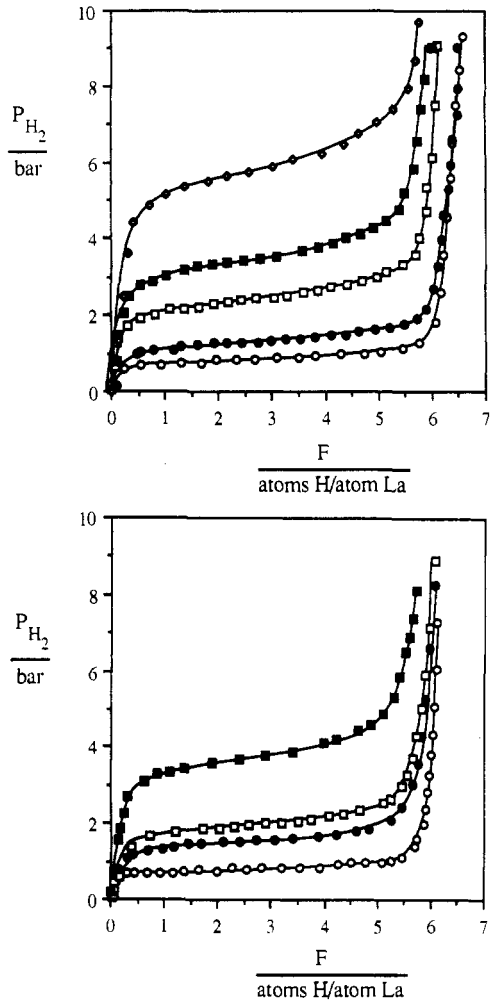

Figure 2. (a, top) Pressure–composition isotherm for $LaNi_{4.8}Al_{0.2}$ absorption: (○) 298 K, (●) 309 K, (□) 323 K, (■) 333 K, (◇) 347 K. (b, bottom) Pressure–composition isotherm for $LaNi_{4.8}Al_{0.2}$ desorption: (○) 308 K, (●) 324 K, (□) 333 K, (■) 348 K.

Parts and and b of Figure 3 illustrate the temperature influence on, respectively, the absorption and desorption equilibrium pressures at $F/F_{max} \approx 0.5$. For $LaNi_{4.5}Al_{0.5}$, $LaNi_{4.6}Al_{0.4}$, and $LaNi_{4.7}Al_{0.3}$ only absorption curves have been measured, since the desorption equilibrium pressures became too low in the temperature range applied. The absorption equilibrium pressures for the last three alloys are also included in Figure 3a. According to Reilly (5), the slope of the curves is equal to the $\Delta H°/R$ of the hydride formation reaction, whereas the intercept is equal to $\Delta S°/R$. Consequently, the equilibrium pressure can be correlated with a van't Hoff relation for absorption:

$$\ln P_{eq} = \frac{\Delta H°}{RT} - \frac{\Delta S°}{R} \qquad (1)$$

In Table 1 the obtained results are summarized. The stability of the hydrides appears to increase (larger $\Delta H°$) at increasing aluminum content. The influence of Al is also shown in Figure 4, in which the absorption equilibrium pressure at $F/F_{max} = 0.5$ is presented as a function of the aluminum content in the alloys (as x in $LaNi_{5-x}Al_x$). The equilibrium pressures have been calculated with the van't Hoff relation and the data in Table 1. The measured equilibrium pressures for $LaNi_{4.9}Al_{0.1}$ are somewhat higher than expected according to the curves in Figures 3a and 4. This can probably be attributed to a different preparation technique employed by the supplier

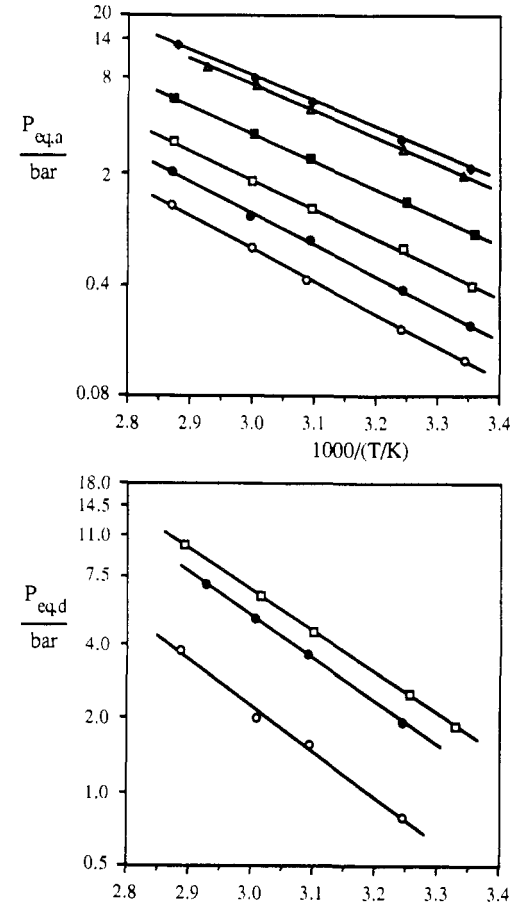

Figure 3. (a, top) absorption equilibrium curves at $F/F_{max} \approx 0.5$: (○) $LaNi_{4.5}Al_{0.5}$, (●) $LaNi_{4.6}Al_{0.4}$, (□) $LaNi_{4.7}Al_{0.3}$, (■) $LaNi_{4.8}Al_{0.2}$, (△) $LaNi_{4.9}Al_{0.1}$ (◆) $LaNi_5$. (b, bottom) Desorption equilibrium curves at $F/F_{max} \approx 0.5$: (○) $LaNi_{4.8}Al_{0.2}$, (●) $LaNi_{4.9}Al_{0.1}$, (□) $LaNi_5$.

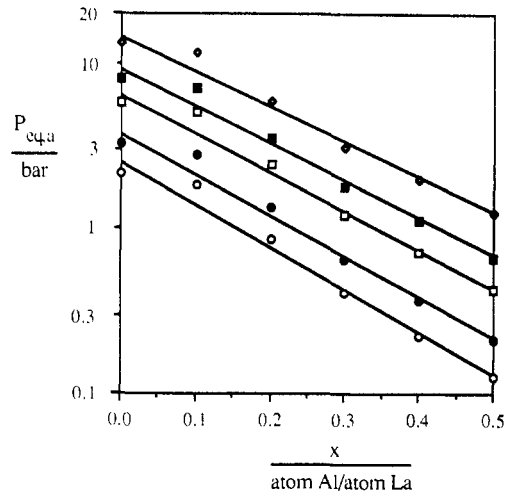

Figure 4. Influence of the aluminum content on the absorption equilibium pressure: (○) 298 K, (●) 308 K, (□) 323 K, (■) 333 K, (◇) 348 K.

of $LaNi_{4.9}Al_{0.1}$ as compared to the method used by the supplier of the other alloys.

2.2. Other Properties of the Metal Alloys. After about 50 absorption/desorption cycles, the particle diameter of the obtained powder reached a stable size. For such powders, the particle size distribution was measured with a laser diffraction particle size distribution analyzer (Horiba LA-500) parts a–c of Figure 5 show results for $LaNi_{4.8}Al_{0.2}$, $LaNi_{4.9}Al_{0.1}$, and $LaNi_5$, respectively. The average particle diameters

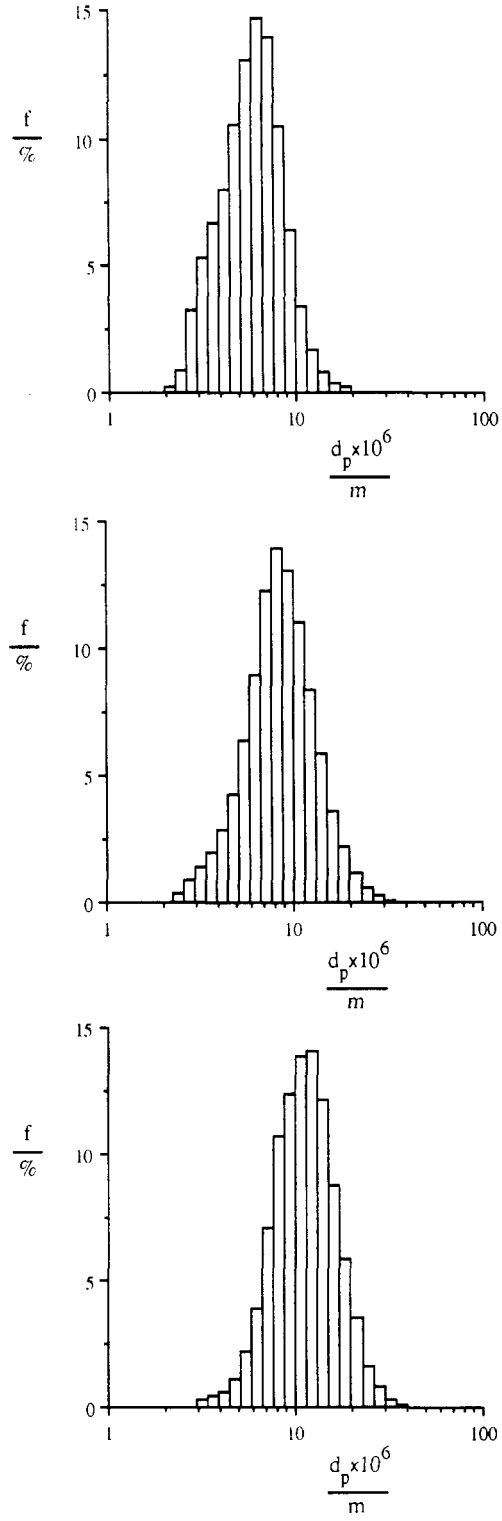

Figure 5. (a, top) Particle size distribution for $LaNi_{4.8}Al_{0.2}$ with d_p = particle diameter and f = volume percentage. (b, middle) Particle size distribution for $LaNi_{4.9}Al_{0.1}$ with d_p = particle diameter and f = volume percentage. (c, bottom) Particle size distribution for $LaNi_5$ with d_p = particle diameter and f = volume percentage.

were derived from the size distribution and are listed in Table 2, together with the surface area of the same powders and the density (ρ_{hydr}) and molecular mass (M_{hydr}) of the materials.

Surface area (A_{hydr}) measurements were performed with nitrogen adsorption at 77 K. Finally, the density of the metal alloys was determined with a pycnometer, using methanol as a solvent. The results show a linear relationship between the

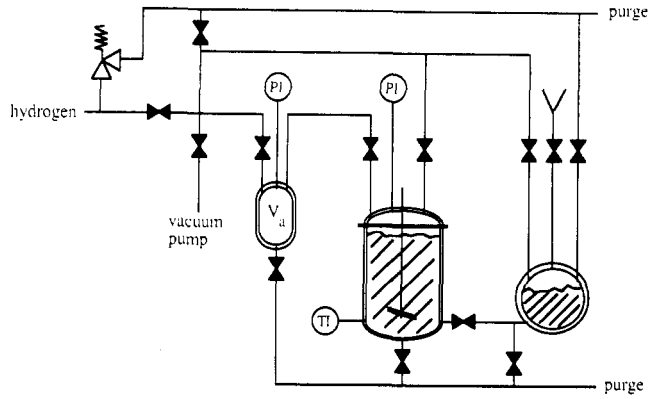

Figure 6. Experimental setup for the determination of hydrogen solubility in a liquid.

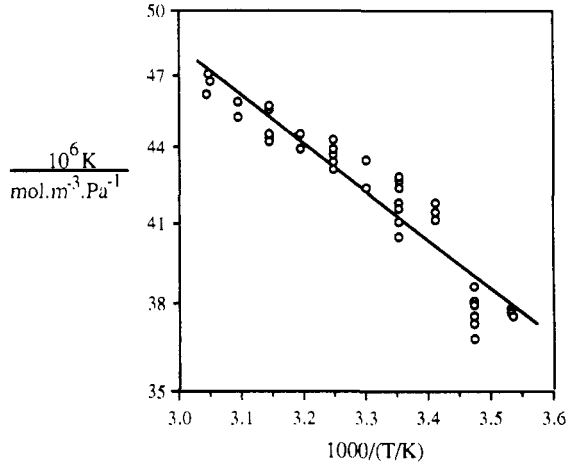

Figure 7. Solubility of hydrogen in cyclohexane.

Table 2. Several Other Properties: Molecular Weight, M, Surface Area of the Metal Hydride Particles, A, Density, ρ, and Particle Diameter, d_p

material	M_{hydr}/ (kg·mol)	A_{hydr}/ ($m^2 \cdot kg^{-1}$)	ρ_{hydr}/ ($kg \cdot m^{-3}$)	$d_p \times 10^6$/m
$LaNi_{4.8}Al_{0.2}$	0.4261	360	8110	6
$LaNi_{4.9}Al_{0.1}$	0.4293	300	8200	9
$LaNi_5$	0.4325	310	8290	11

density (kg/m^3) and the aluminum mole fraction (x) in the alloys according to

$$\rho_{hydr} = 8290 - 904x \quad \text{with} \quad 0 \le x \le 0.5 \qquad (2)$$

The data in Table 2 are calculated according to eq 2.

3. Properties of the Solvents

The solubility of hydrogen in cyclohexane has been determined using the experimental arrangement shown in Figure 6. The gas + liquid equilibrium cell is a stirred vessel (V = 99 cm^3), which is connected to storage vessels for hydrogen (V_a = 220 cm^3) and cyclohexane. The temperatures (kept constant within ±0.05 K) of all three vessels are identical. Prior to the absorption of hydrogen, the liquid was completely degassed and the vapor pressure was measured. After filling the hydrogen storage vessel with pure hydrogen, the pressure was recorded. The valve between the hydrogen storage vessel and the equilibrium cell was then opened till both pressures were equal and closed again, after which the stirrer was started. The stirring was stopped after equilibrium between the gas and liquid phase had been established, and the pressure in the equilibrium cell and hydrogen storage vessel were recorded. With the measured pressures, temperature, amount

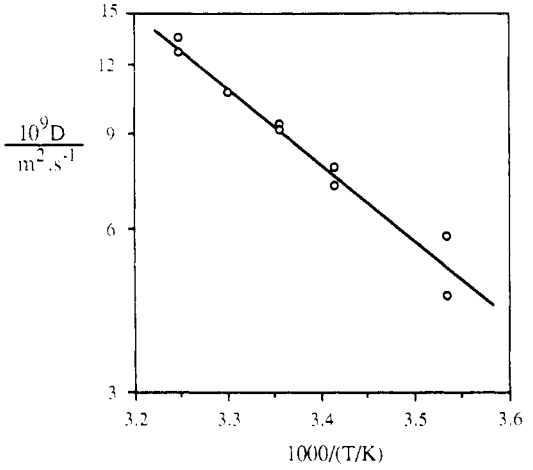

Figure 8. Diffusion coefficient of hydrogen in cyclohexane.

of cyclohexane in the equilibrium cell, and gas volumes of the two vessels, the hydrogen solubility in cyclohexane were determined, expressed by m_{H_2} which is a solubility coefficient defined as

$$m_{H_2} = C_{H_{2,l}}/C_{H_{2,g}} \quad (3)$$

where $C_{H_{2,l}}$ and $C_{H_{2,g}}$ are the hydrogen concentrations in the liquid phase and gas phase at equilibrium, respectively.

Figure 7 shows the experimental results for the absorption of hydrogen in cyclohexane; the solubility has been presented as a Henry coefficient, K, which is directly related to the solubility coefficient according to $K = m/(RT)$, with $R = 8.314$ $Pa \cdot m^3 \cdot K^{-1} \cdot mol^{-1}$. The results are correlated with eq 4. The Henry coefficient of hydrogen in ethanol has been calculated with data provided by Clever (*6*) for temperatures between 293 and 333 K. The following relations have been obtained by means of the least-squares method:

$$K_{H_2} = 189 \times 10^{-6} \exp\{-454.0/(T/K)\} \text{ in cyclohexane} \quad (4)$$

$$K_{H_2} = 101 \times 10^{-6} \exp\{-317.5/(T/K)\} \text{ in ethanol} \quad (5)$$

The diffusion coefficient of hydrogen in cyclohexane, D, is measured in a diaphragm cell as described by Littel *et al.* (*7*). The results are presented in Figure 8 and have been correlated with

$$D_{H_2} = 4.780 \times 10^{-4} \exp\{-3239/(T/K)\} \quad (6)$$

Acknowledgment

We acknowledge E. Damhuis, M. Engman, M. v.d. Horst, and W. Starmans for their contribution to the experimental work and K. van Bree, S. Kuipers, A. H. Pleiter, and G. Schorfhaar for their technical support.

Literature Cited

(1) Buschow, K. H. J.; van Mal, H. H. *J. Less-Common Met.* **1972**, *29*, 203.
(2) Mendelsohn, M. H.; Gruen, D. M.; Dwight, A. E. *Adv. Chem. Ser.* **1979**, *173*, 279.
(3) Snijder, E. D.; Versteeg, G. F.; van Swaaij, W. P. M. The Kinetics of hydrogen absorption and desorption in $LaNi_{5-x}Al_x$ slurries. *AIChE J.* **1993**, *39* (9), 1444.
(4) Snijder, E. D.; Versteeg, G. F.; van Swaaij, W. P. M. *Chem. Eng. Sci.* **1993**, *48*, 2429.
(5) Reilly, J. J., Metal hydrides as hydrogen storage media and their applications. In *Hydrogen, its technology and implications*; Cox, K. E., Williamson, K. D., Eds.; CRC Press: Cleveland, 1977; Vol. 2, p 13.
(6) Clever, H. L. Solubility data series, hydrogen and deuterium. In *International Union of Pure and Applied Chemistry*; Young, C. L., Ed.; Pergamon Press: Oxford, 1981.
(7) Littel, R. J.; Versteeg, G. F.; van Swaaij, W. P. M. *J. Chem. Eng. Data* **1992**, *37*, 42.

Received for review October 20, 1992. Revised August 5, 1993. Accepted January 21, 1994.® These investigations were supported by the Foundation for Chemical Research in the Netherlands (SON) and by DSM.

® Abstract published in *Advance ACS Abstracts*, March 1, 1994.